Electronic Supplementary Material (ESI) for Journal of Materials Chemistry A.

Supplementary Information

Large-scale Fabrication of Heavy Doped Carbon Quantum Dots with Tunable-photoluminescence and Sensitive Fluorescent Detection

Experimental Section

^{1}H NMR and ^{13}C NMR spectra were acquired at 600 MHz (DMSO-d_6) on a Bruker DRX500 spectrometer. NMR chemical shifts are expressed relative to TMS as the internal standard.

NMR analysis

Lampblack
^{1}H-NMR: no signal of H in the spectrum of lampblack
^{13}C-NMR: δ 31.18 (aryl group)
Oxidized-CQDs
^{1}H-NMR: δ 1.25 (m CH_2), 2.50 (s CH_3), 3.45 (d CH), 4.24 (q, 7^6 Ar-O-CH_3), 4.71 (s -OH), 8.32 (s CH)
^{13}C-NMR: δ 14.17 (C=O), 31.18 (aryl group), 62.51 (C=O), 68.82 (COOH), 75.03 (C-O-C), 118.40 (furan structure), 153.39 (Ar-COOH), 171.13 (R-COOH)
CQDs
^{1}H-NMR: δ 2.43 (s CH_3), 2.67 (m CH_2), 3.94 (sept, 6 CH)
^{13}C-NMR: δ 31.18 (aryl group), 153.39 (Ar-COOH)
N-CQD
^{1}H-NMR: δ 1.71 (m CH_2 cyclohexanone), 5.70 (m CH propylene), 6.25 (m CH(3, 4) pyrrole), 6.69 (m CH(2, 5) pyrrole), 7.06 (s CH (4, 5) imidazole), 7.18 (m CH (2, 4, 6) Ph-CH_3), 7.39 (m CH (3, 5) pyridine), 7.59 (m Ph-CHO)
^{13}C-NMR: δ 21.26 ($N(CH_3)_2$) 24.35 (CH_2 cyclohexanone), 29.38 (CH_3CO), 31.18 (aryl group), 62.21 (C-O-C), 107.82 (CH pyrrole), 116.07 (CH_2 propylene), 122.79 (CH(4,5) imidazole), 123.14 (CH(3,5) pyridine), 126.56 (Ph-CH_3), 134.63 (CH imidazole), 145.16 (Ar-COOH)
S-CQDs
^{1}H-NMR: δ 2.50 (s CH_3), 2.91 (s SH), 7.15 (m CH(2,4,6) Ph-CH_3), 7.57 (m CH(3,5) Ph-CH_3)
^{13}C-NMR: δ 31.18 (aryl group), 126.21 (Ph-S), 127.56 (Ph-C=O)
Se-CQDs
^{1}H-NMR: δ 2.50 (s CH_3), 6.78 (s ArH), 7.34 (s CH benzene), 7.63 (m CH Ph-R), 9.32 (s Ph-SeH)
^{13}C-NMR: δ 31.18 (aryl group), 128.33 (CH benzene), 129.99 (CH Ar-Se), 131.29 (C Ar)

Fig and Table

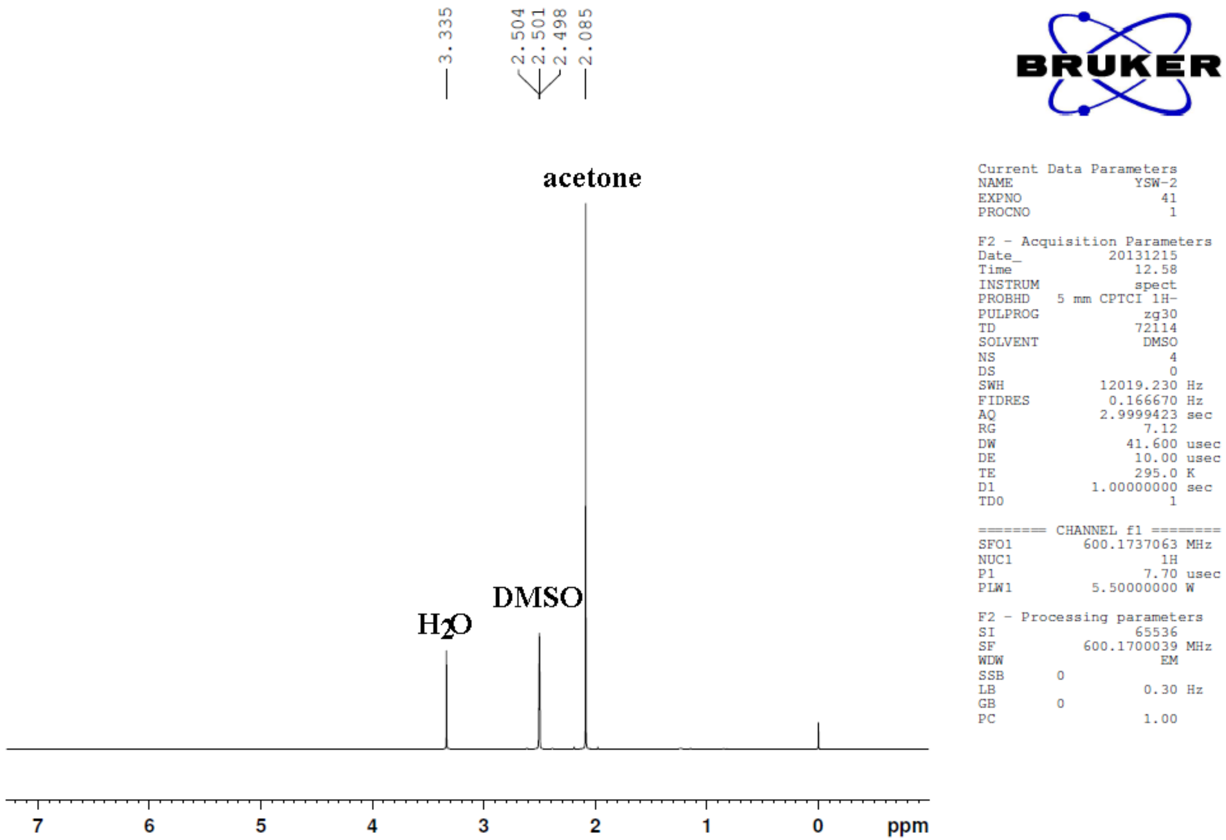

Fig. S1 ^{1}H-NMR spectrum of lampblack

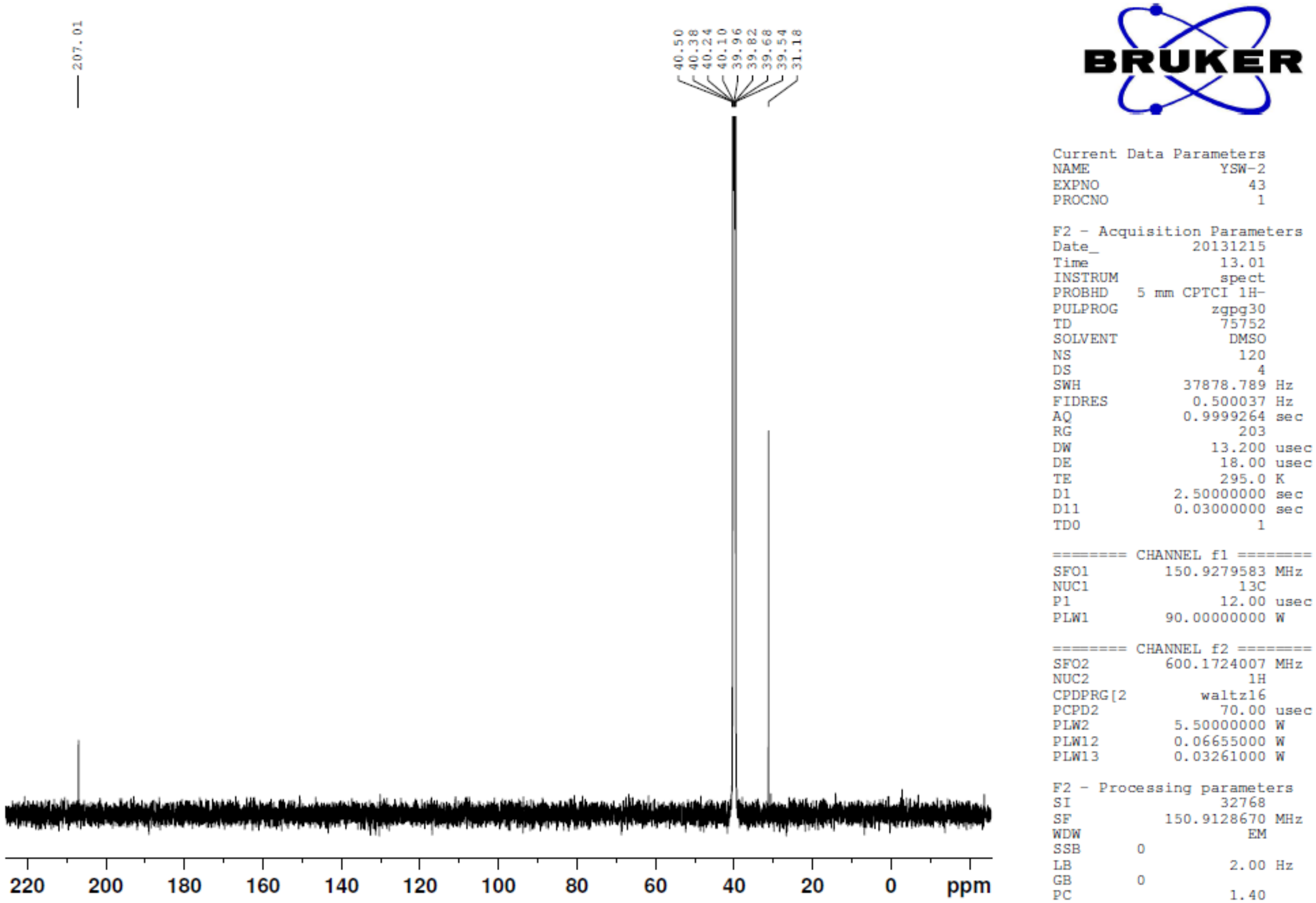

Fig. S2 ^{13}C-NMR spectrum of lampblack

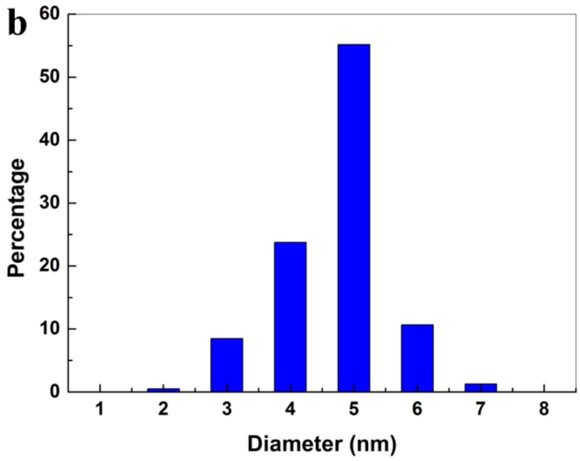

Fig. S3 the corresponding size distribution histogram of oxidized CQDs

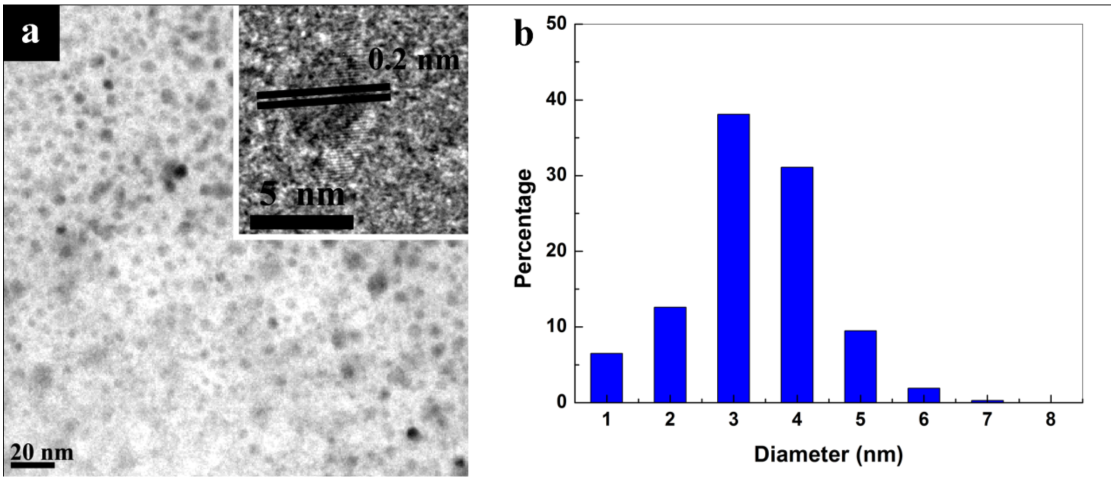

Fig. S4 (a) TEM images of the N-CQDs thus formed with the inset of HRTEM image; (b) the corresponding size distribution histogram.

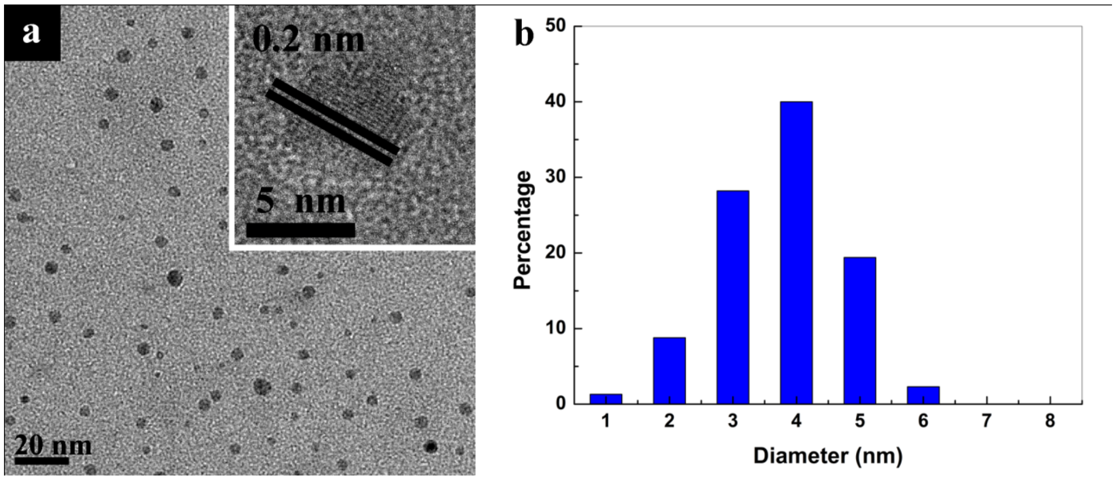

Fig. S5 (a) TEM images of the S-CQDs thus formed with the inset of HRTEM image; (b) the corresponding size distribution histogram.

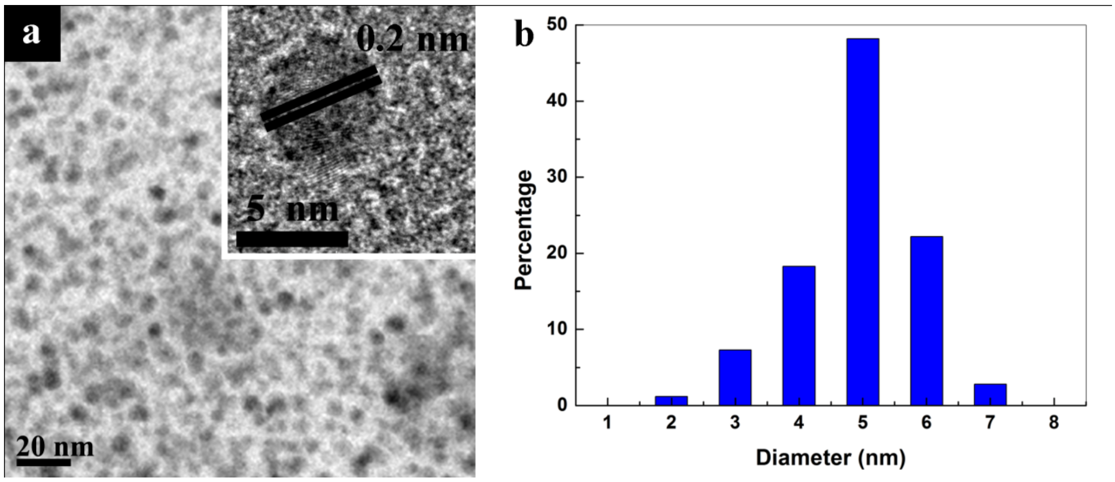

Fig. S6 (a) TEM images of the Se-CQDs thus formed with the inset of HRTEM image; (b) the corresponding size distribution histogram.

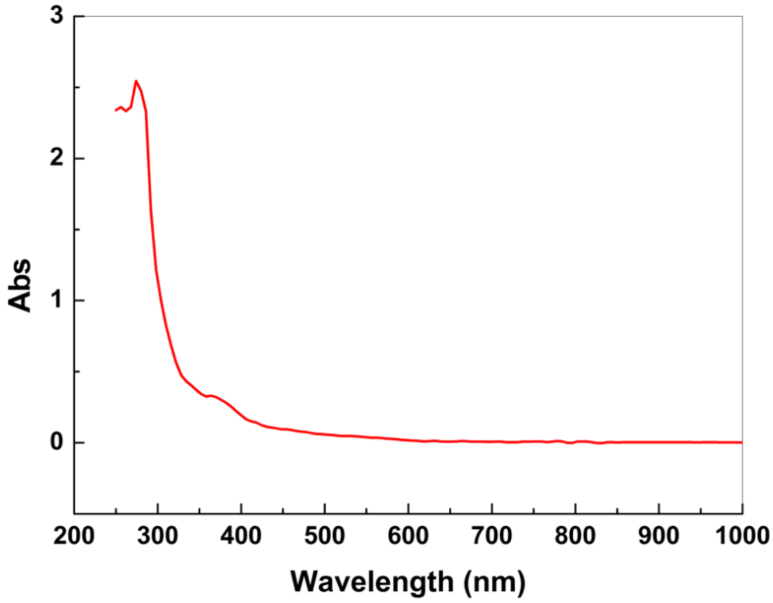

Fig. S7 UV-vis spectrum of S-CQDs at room temperature.

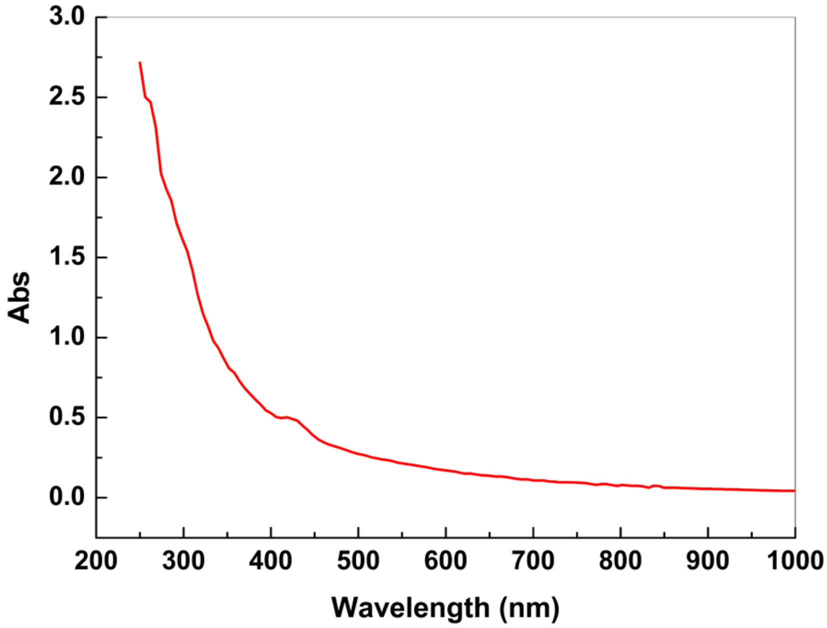

Fig. S8 UV-vis spectrum of Se-CQDs at room temperature.

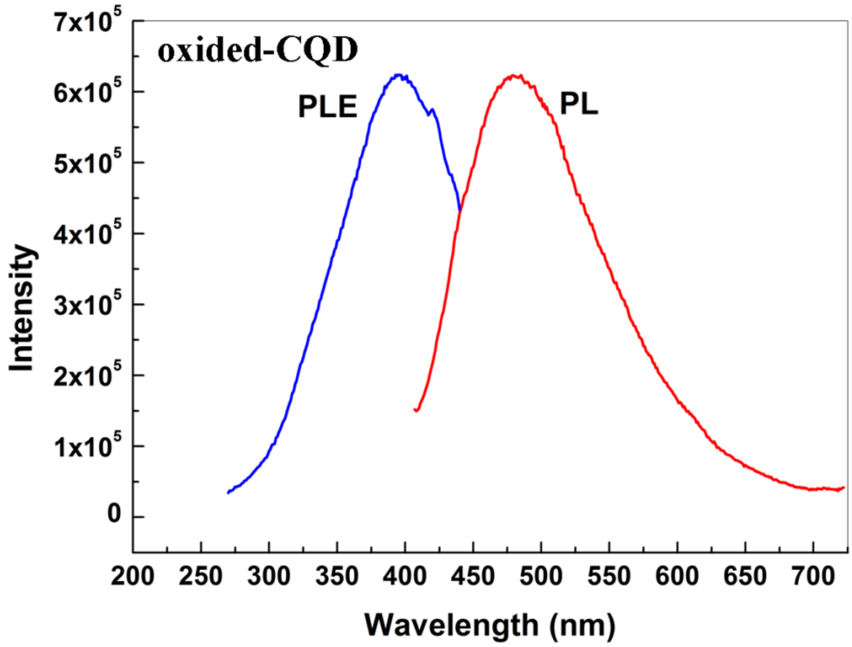

Fig. S9 PLE spectrum of oxidized-CQDs with emission at 482 nm and PL spectrum of the blue oxidized-CQDs excited at 397 nm registered at room temperature.

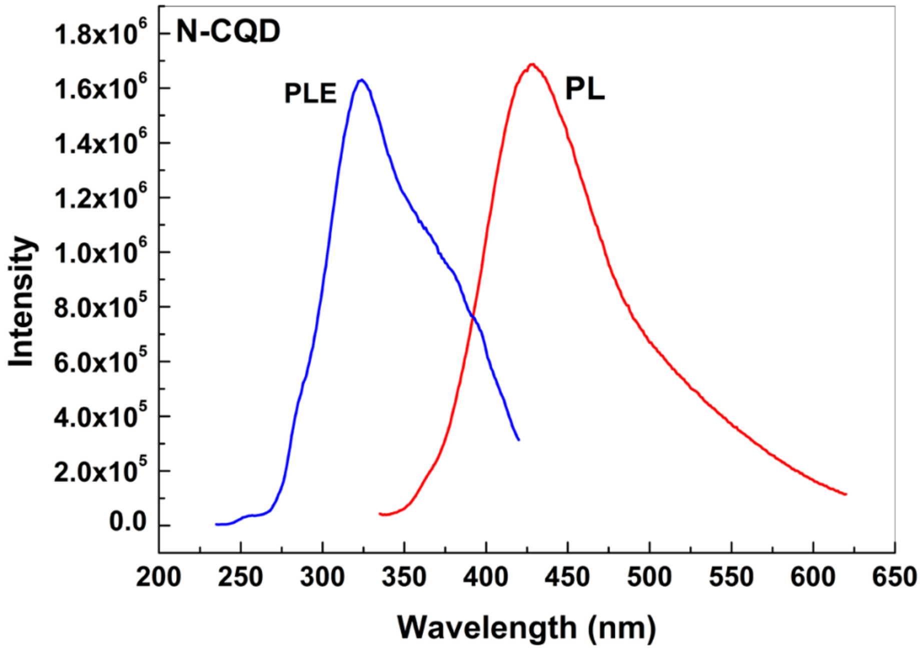

Fig. S10 PLE spectrum of N-CQDs with emission at 428 nm and PL spectrum of the blue oxidized N-CQDs excited at 324 nm registered at room temperature.

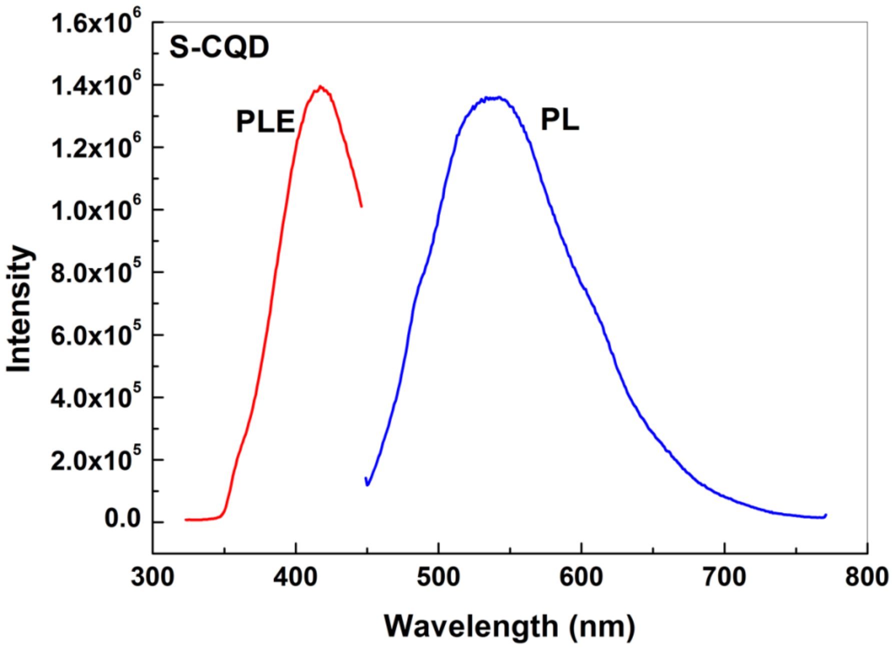

Fig. S11 PLE spectrum of S-CQDs with emission at 539 nm and PL spectrum of the blue oxidized S-CQD excited at 418 nm registered at room temperature.

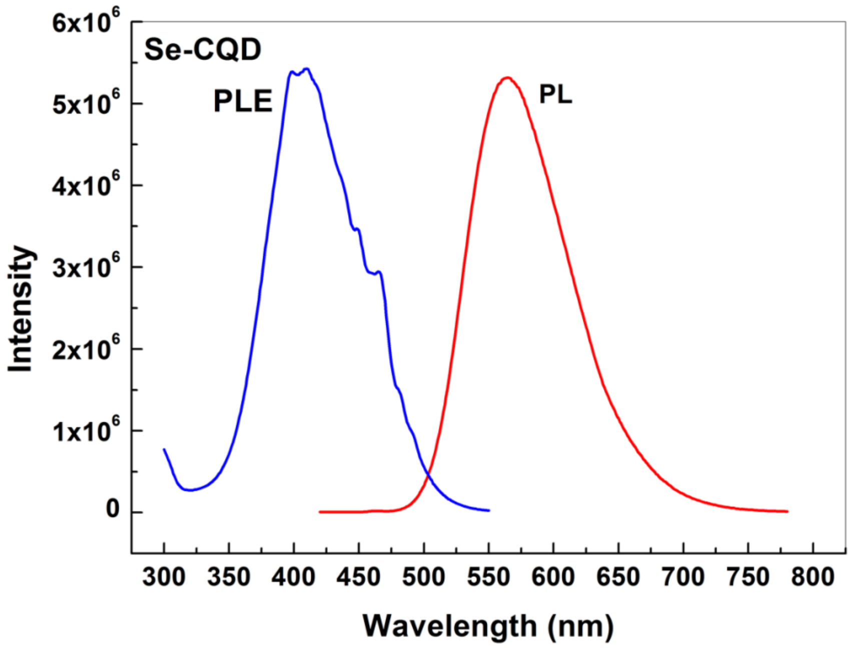

Fig. S12 PLE spectrum of Se-CQDs with emission at 563 nm and PL

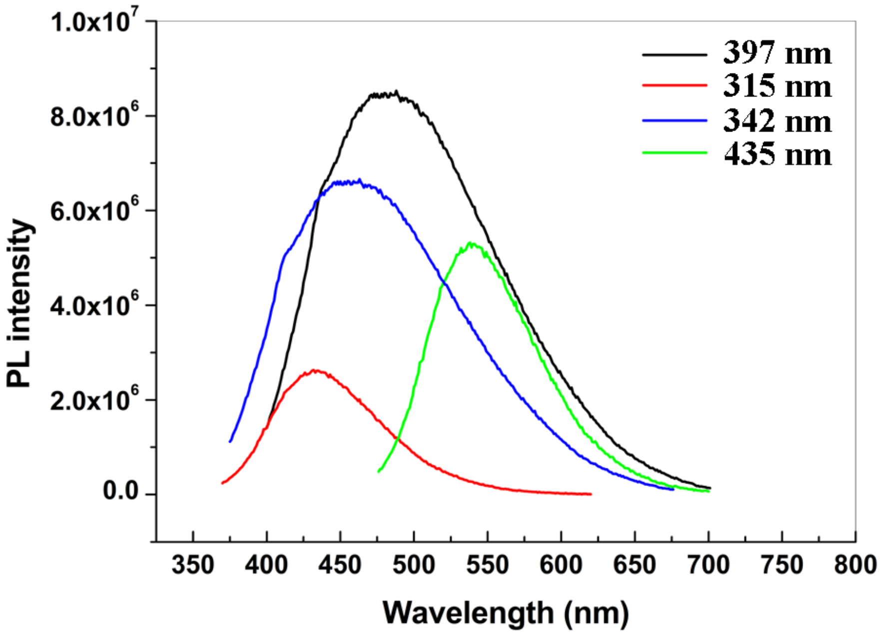

Fig. S13 PL emission spectra of oxidized-CQDs with different excitation wavelength.

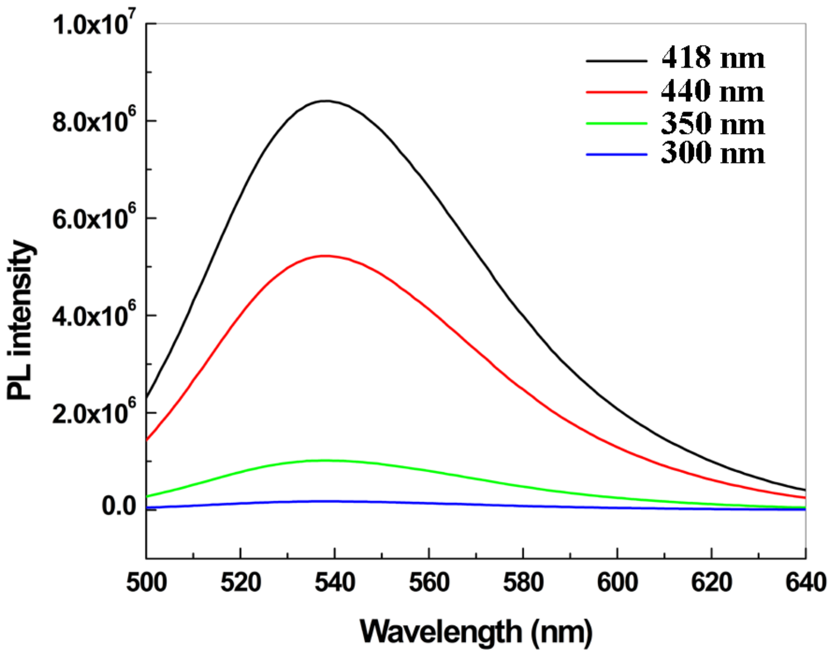

Fig. S14 PL emission spectra of S-CQDs with different excitation wavelength.

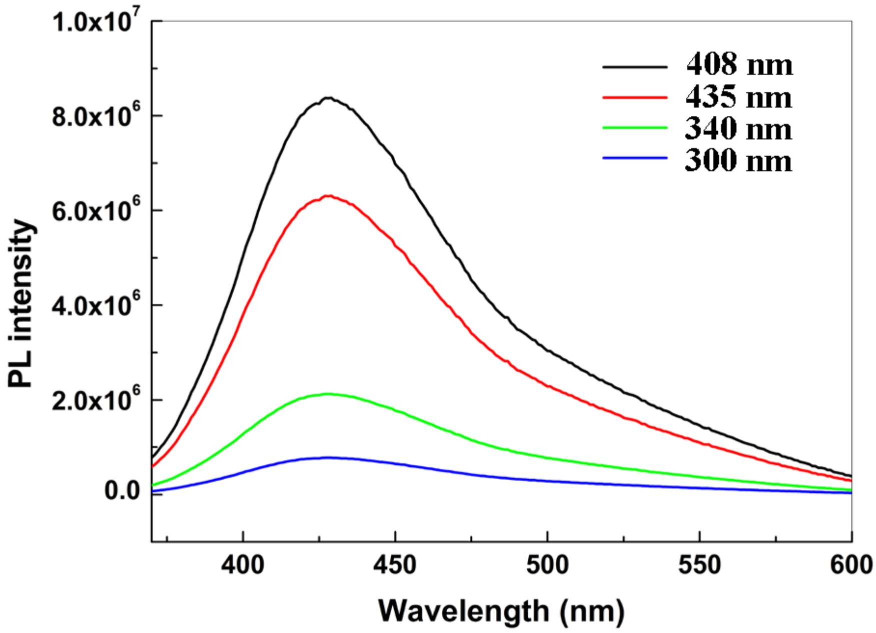

Fig. S15 PL emission spectra of Se-CQDs with different excitation wavelength.

Table S1. Quantum yield (Φ_f) Comparison of different CQDs

CQDs	**Quantum yield (Φ_f)**	**Ref.**
CQDs	0.12 [a]	7
CQDs	0.04-0.1 [b]	4
CQDs	0.47 [b]	11
CQDs	0.15 [b]	11
CQDs	0.24 [b]	11
N-CQDs	0.025 [b]	13
N-CQDs	0.062 [b]	13
CQDs	0.069 [b]	18
CQDs	0.26 [b]	16
CQDs	0.0322 [b]	17
CQDs	0.24 [b]	28
Passivated CQDs	0.2 [b]	S1
N-CQDs	0.39 [b]	This work
S-CQDs	0.24 [b]	This work
Se-CQDs	0.19 [a]	This work

[a] calibrating against rhodamine B in ethanol.
[b] calibrating against quinine sulfate in 0.10 M H_2SO_4 solution.

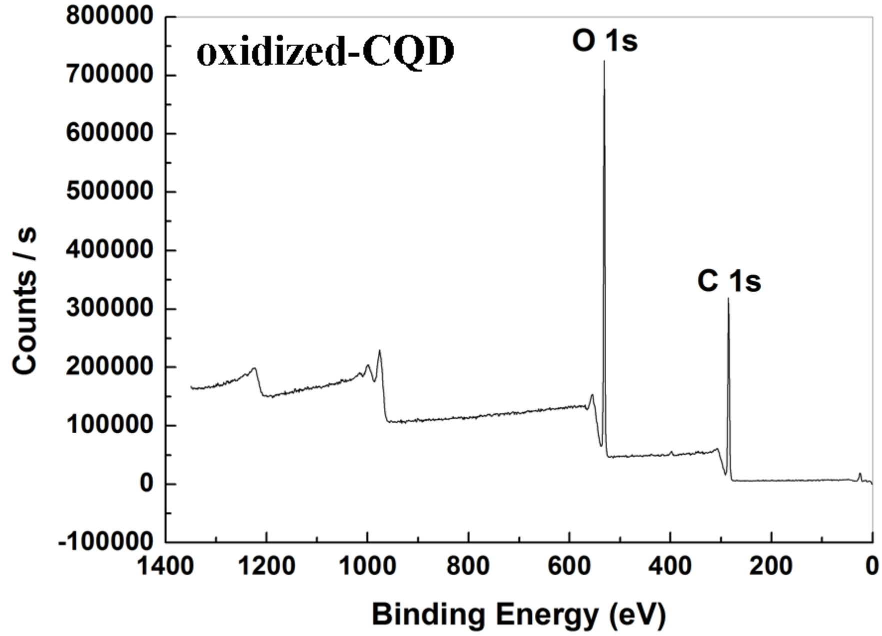

Fig. S16 Survey XPS spectrum of oxidized-CQDs

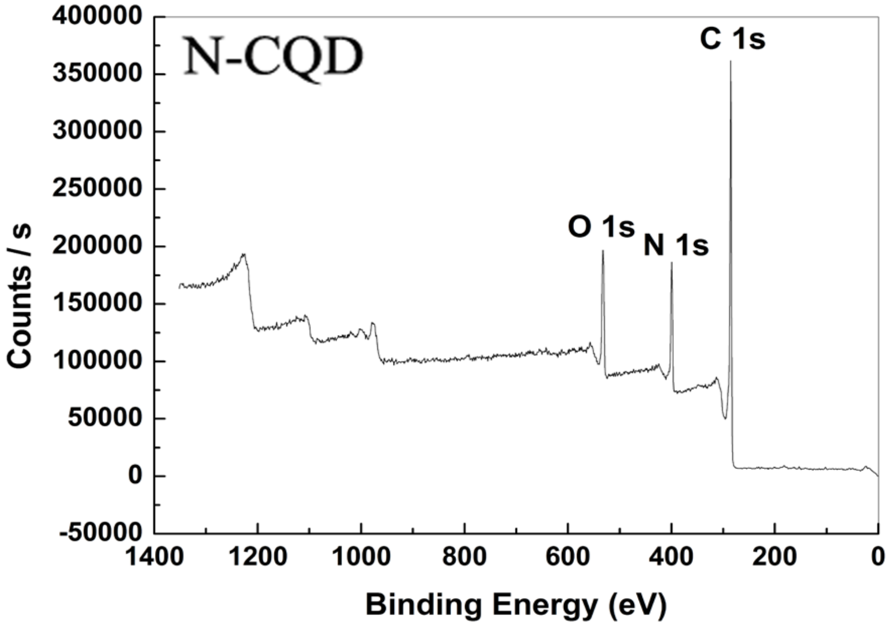

Fig. S17 Survey XPS spectrum of N-CQDs

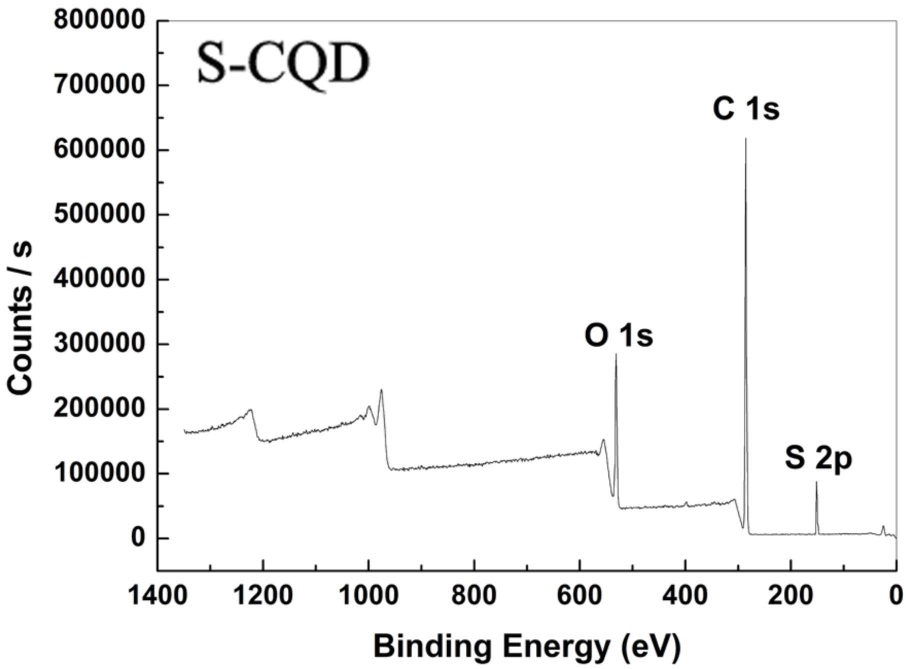

Fig. S18 Survey XPS spectrum of S-CQDs

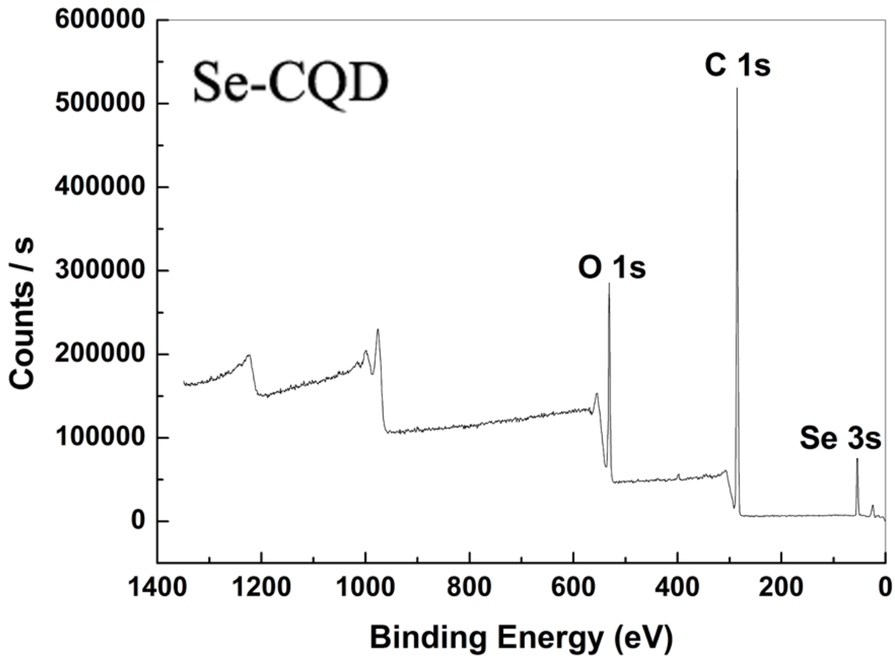

Fig. S19 Survey XPS spectrum of Se-CQDs

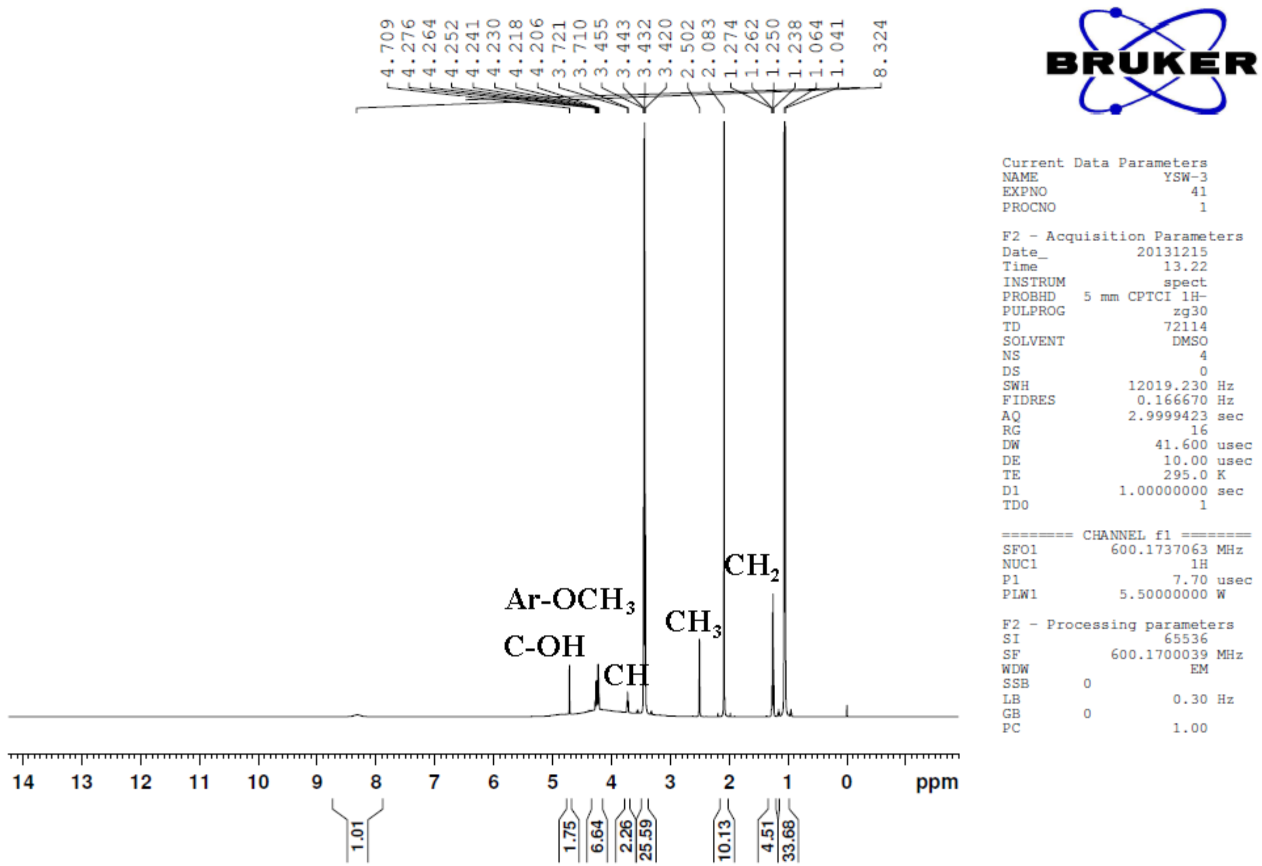

Fig. S20 ^{1}H-NMR spectrum of oxidized-CQDs

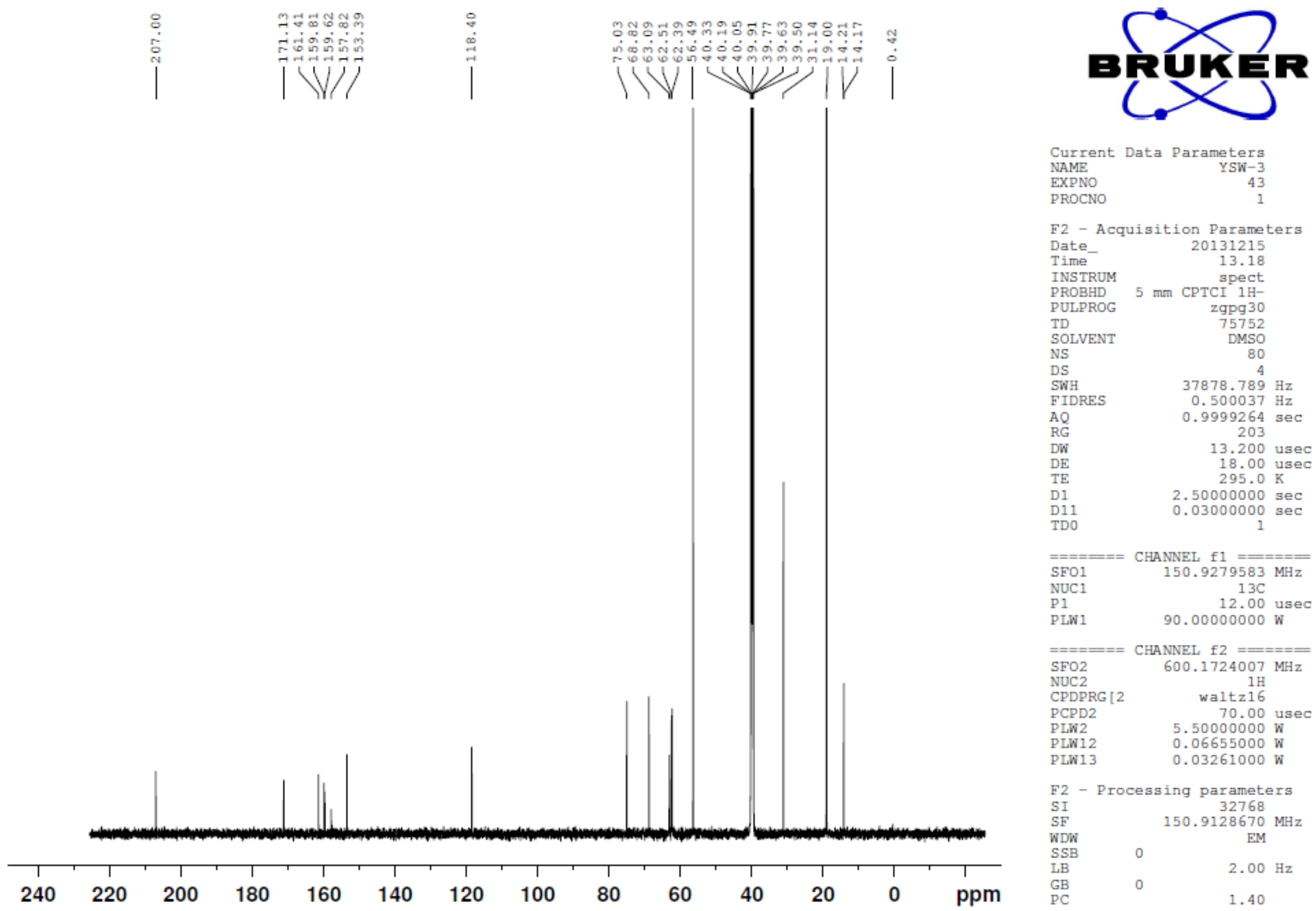

Fig. S21 ^{13}C-NMR spectrum of oxidized-CQDs

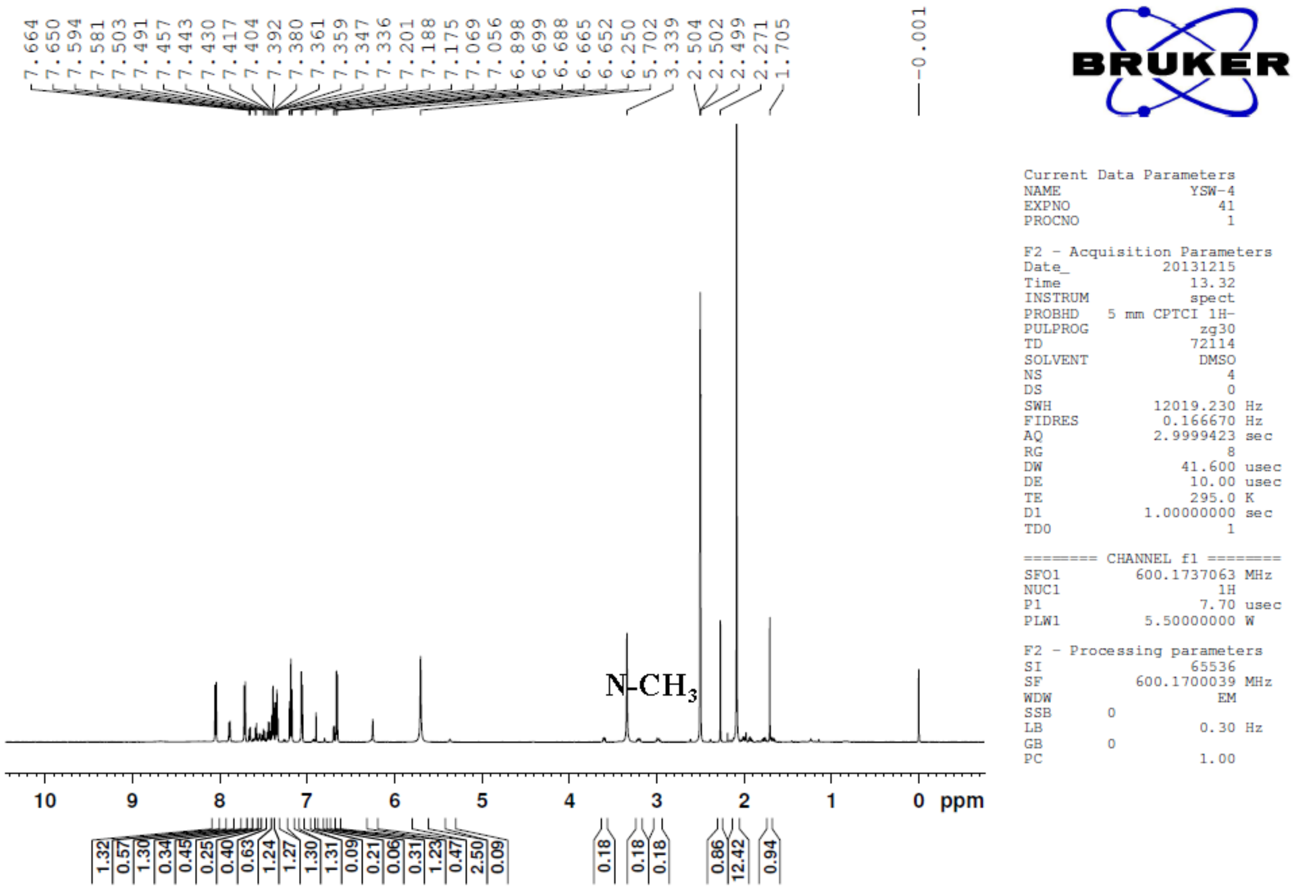

Fig. S22 ^{1}H-NMR spectrum of N-CQDs

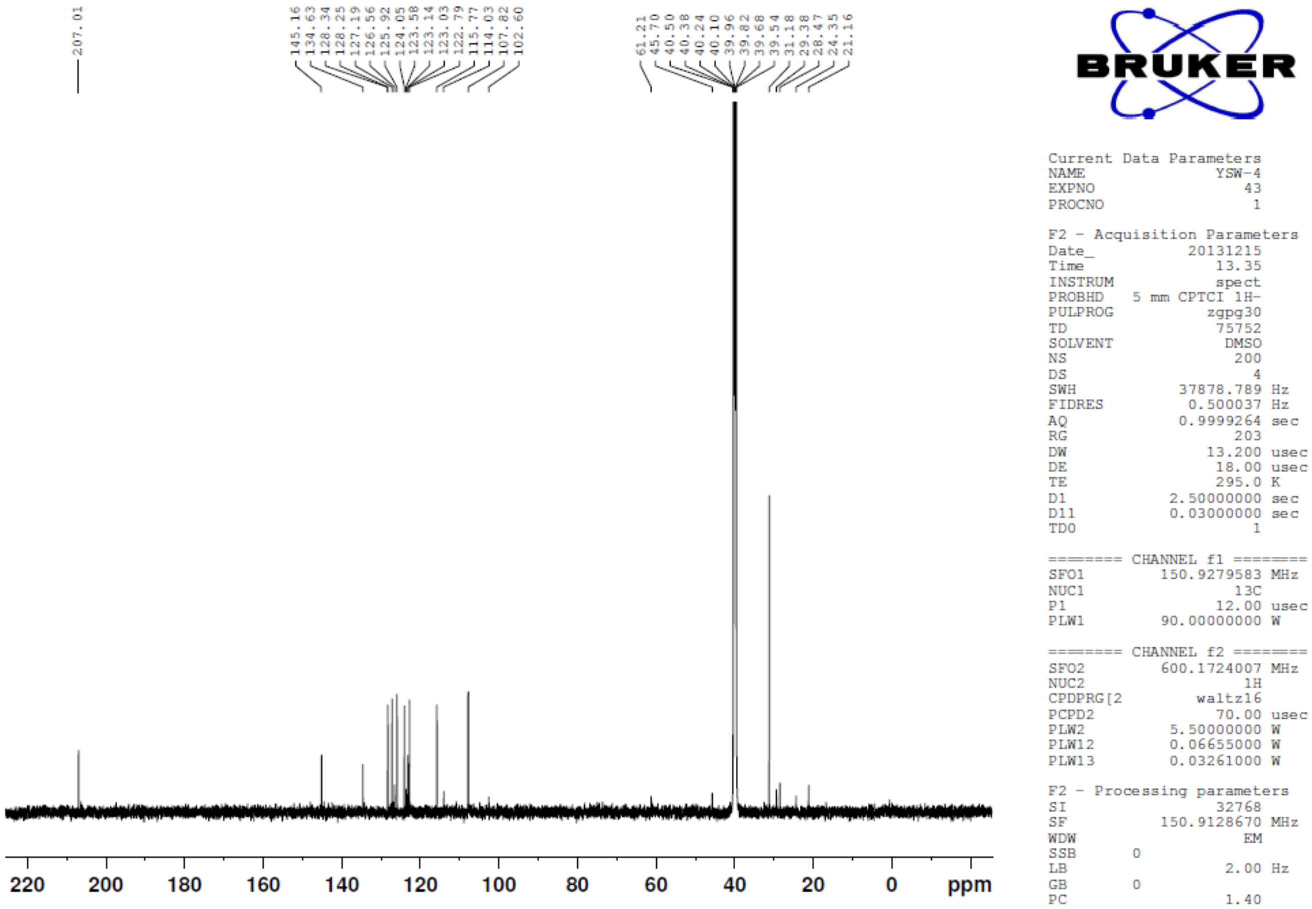

Fig. S23 ^{13}C-NMR spectrum of N-CQDs

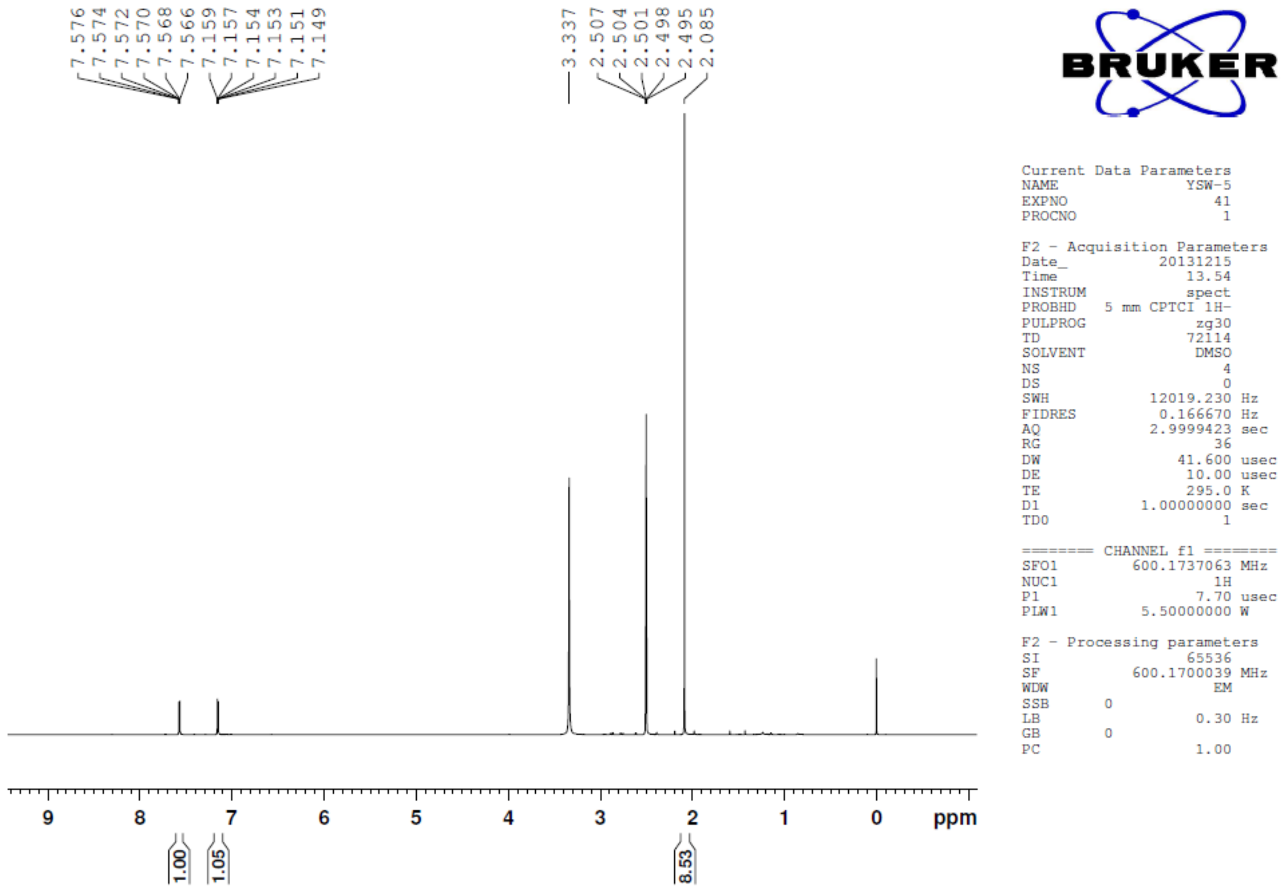

Fig. S24 ^{1}H-NMR spectrum of S-CQDs

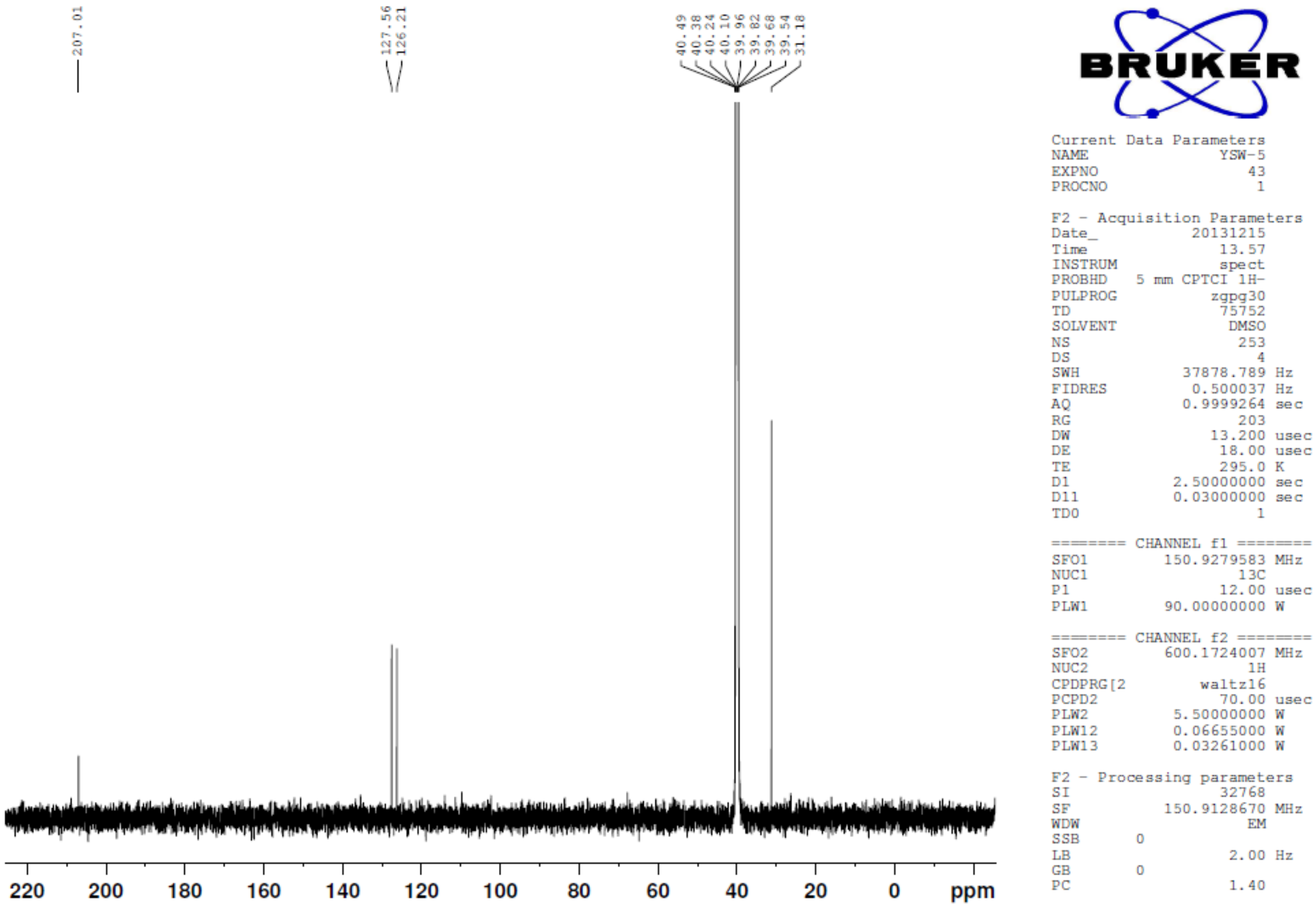

Fig. S25 ^{13}C-NMR spectrum of S-CQDs

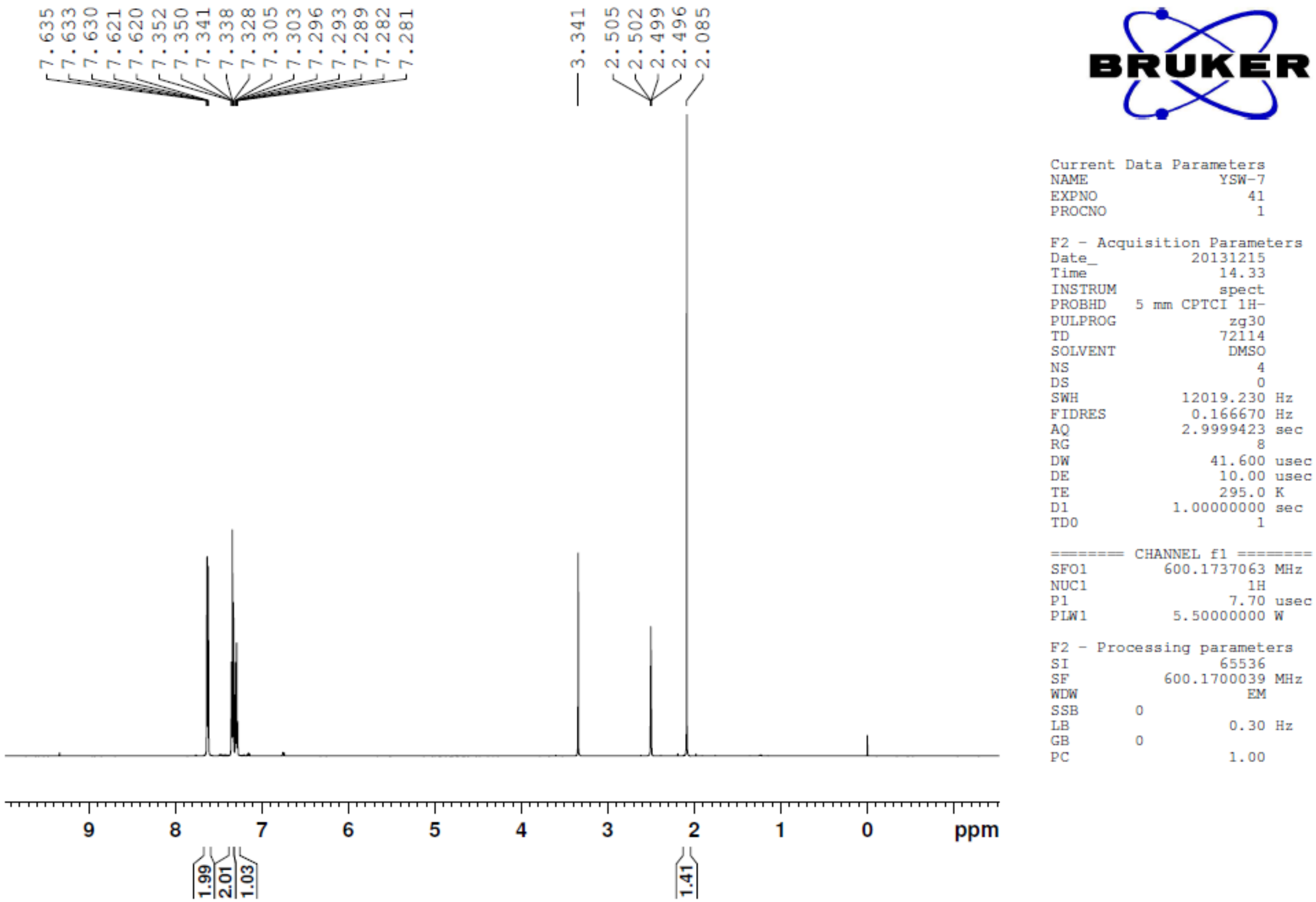

Fig. S26 ^{1}H-NMR spectrum of Se-CQDs

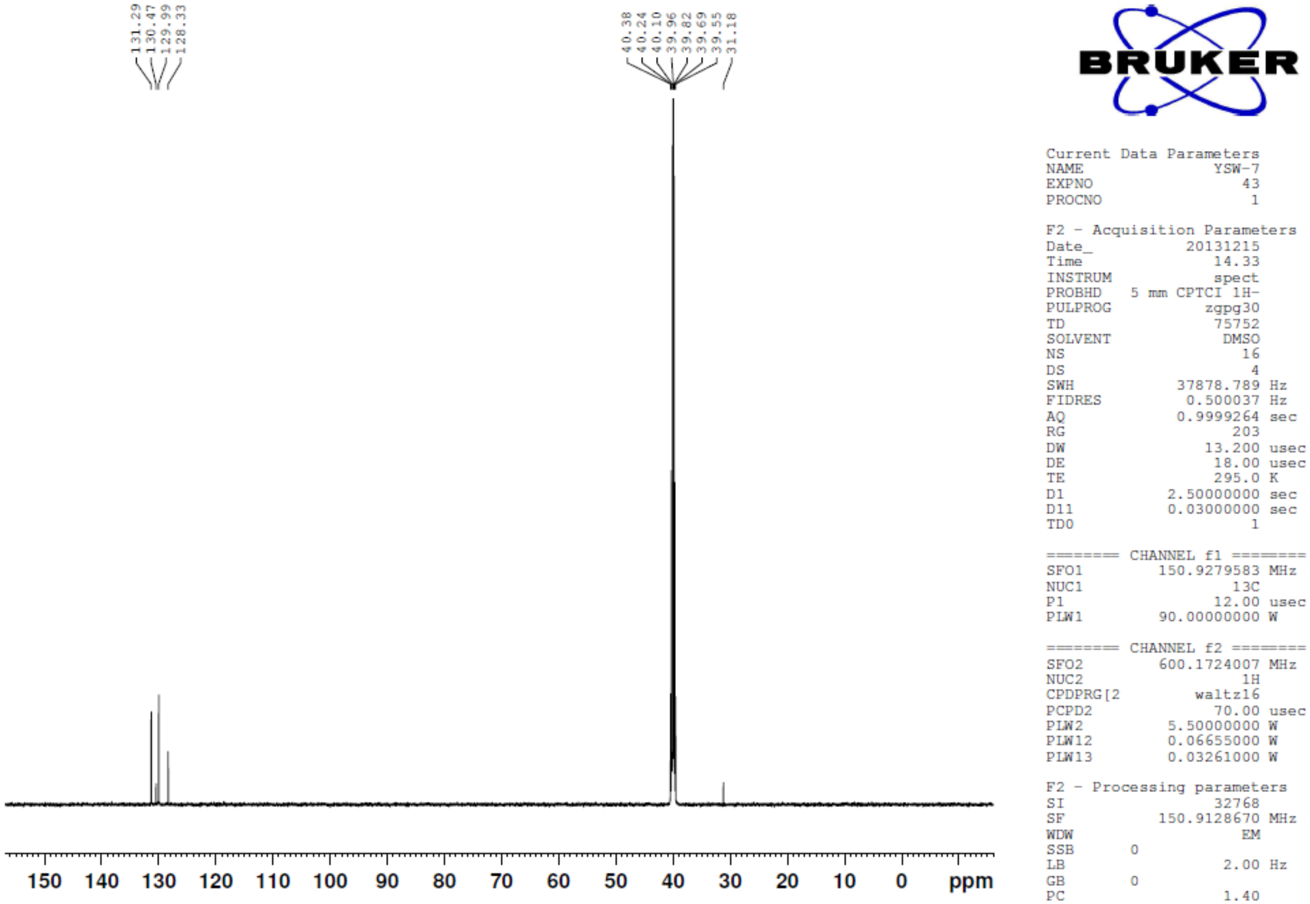

Fig. S27 ^{13}C-NMR spectrum of Se-CQDs

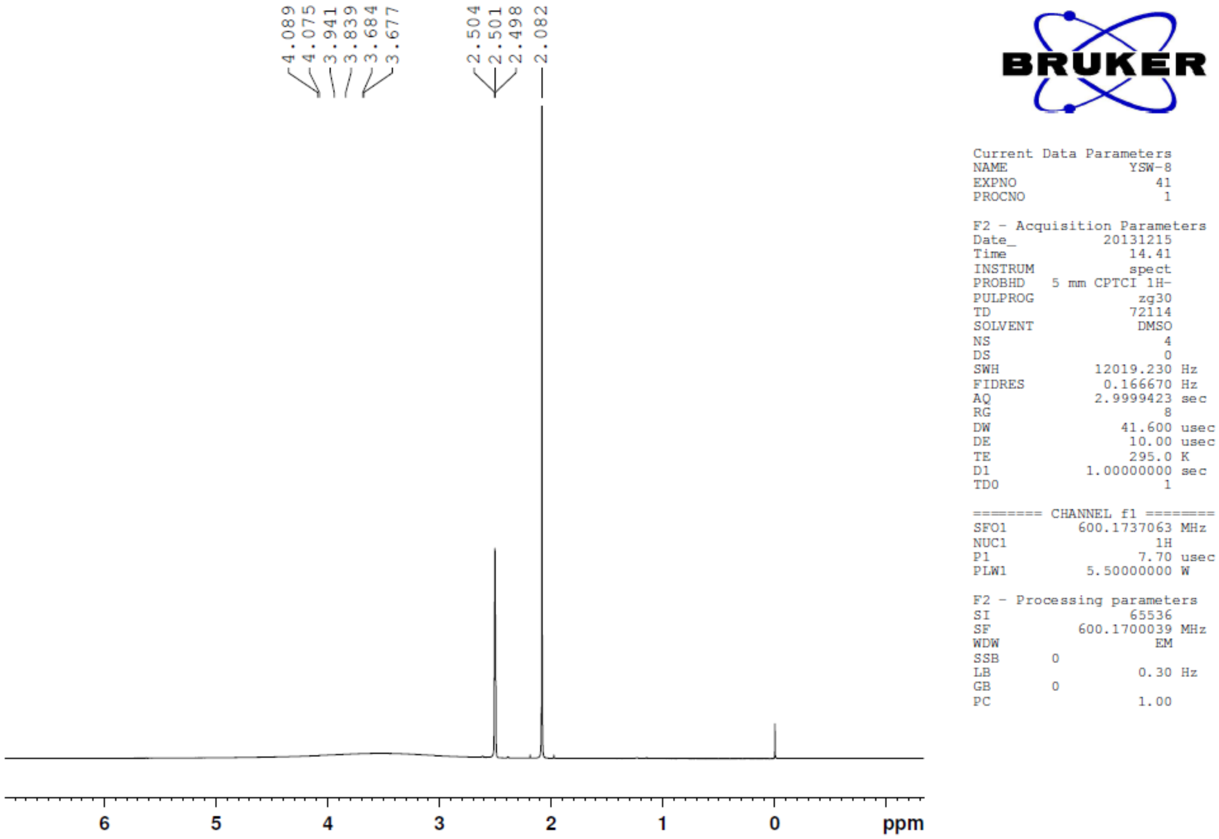

Fig. S28 ^{1}H-NMR spectrum of VC-reduced CQDs

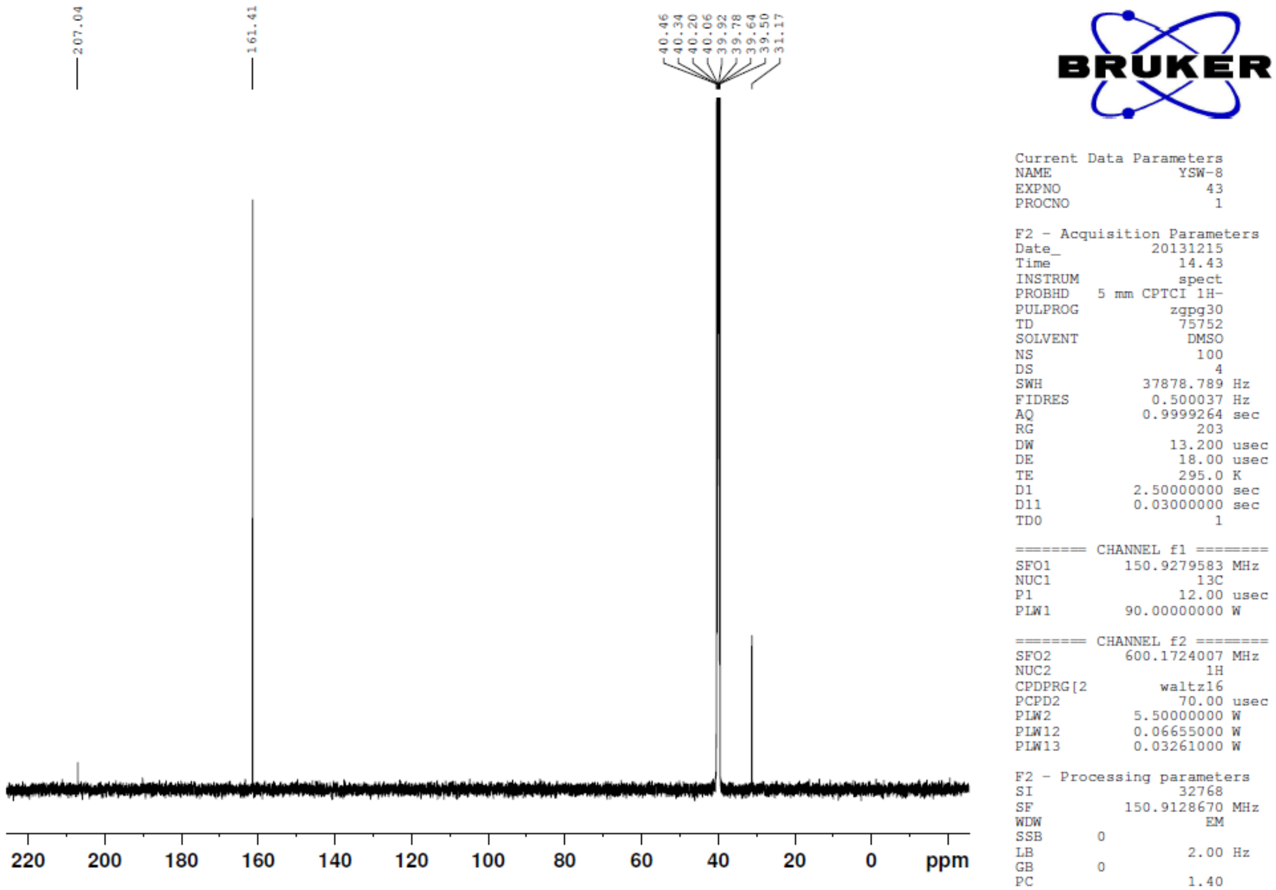

Fig. S29 ^{13}C-NMR spectrum of VC-reduced CQDs

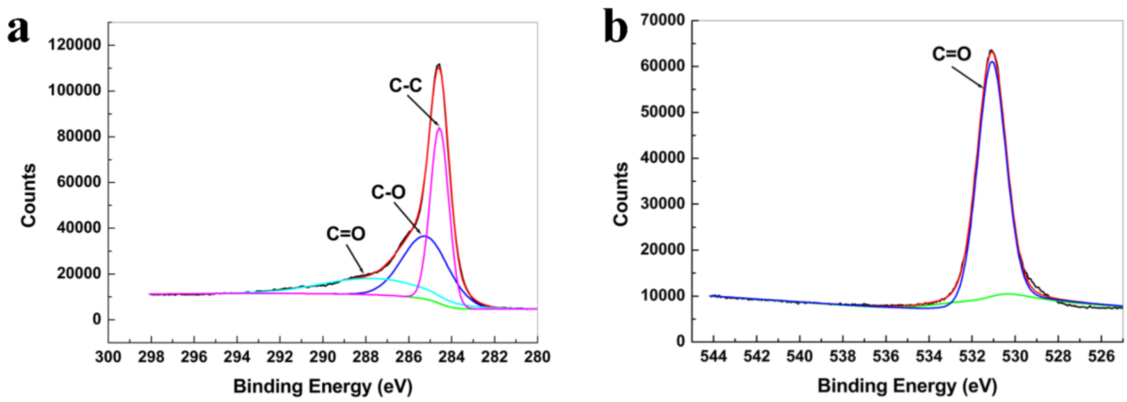

Fig. S30 (a) C1s spectra of CQDs; (b) O1s spectra of VC-reduced CQDs

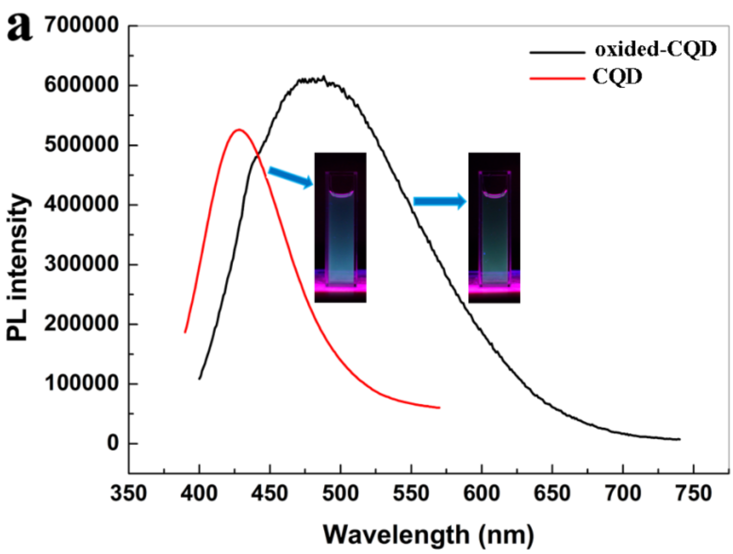

Fig. S31 PL emission spectra of oxidized-CQDs and VC-reduced CQDs

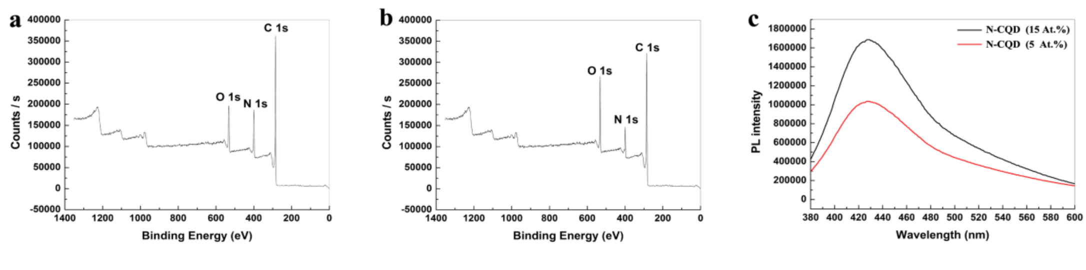

Fig. S32 XPS of N-CQDs with different doping concentrations (a) 15 at.%, (b) 5 at.%. (c) PL emission spectra of N-CQDs with different doping concentrations. The concentrations of all samples are the same (0.5 mg mL^{-1}). The PL emission spectra were measured at room temperature and PBS buffer (pH=7.0).

Table S2. Comparison of different fluorescent probes for Hg^{2+} detection.

Fluorescent probes	Performance		Ref.
	Detection Limit (nM)	Linear range (μM)	
rhodamine thiospirolactam derivative	3	0.01-1	S2
tris[2-(2-aminoethylthio)ethyl]amine	115	0.130-0.360	S3
fluorescent gold nanoparticles	5	0.01-10	S4
fluorescent Ag clusters	10	0.01-5	S5
Au@Ag core-shell nanoparticles	9	0.01-0.45	S6
CdS-encapsulated DNA	4.3	0.01-0.11	S7
CdTe quantum dots	1.55	0.002-0.014	S8
Lys VI-AuNCs	0.003	0.01-5	S9
S-CQD	2	0.002-2	This work

Table S3. Comparison of different CQDs for yield and throughput.

Product	Yield (%)	Throughput/ batch (g)	Ref.
CQD	1	0.4	S10
CQD	-	6.2	S11
CQD	-	1	S12
Oxidized-CQD	80	120	This work
N-CQD	73	13	This work
S-CQD	69	12	This work
Se-CQD	61	11	This work

References

[S1] X. Yu, J. Liu, Y. Yu, S. Zuo, B. Li, Preparation and visible light photocatalytic activity of carbon quantum dots/TiO_2 nanosheet composites, *Carbon*, 2014, **68**, 718.

[S2] S.-T. Yang, X. Wang, H. Wang, F. Lu, P. G. Luo, L. Cao, M. J. Meziani, J.-H. Liu, Y. Liu, M. Chen, Y. Huang, Y.-P. Sun, Carbon Dots as Nontoxic and High-Performance Fluorescence Imaging Agents, *J. Phys. Chem. C*, 2009, **113**, 18110.

[S3] Y.-J. Gong, X.-B. Zhang, Z. Chen, Y. Yuan, Z. Jin, L. Mei, J. Zhang, W. Tan, G.-L. Shena and, R.-Q. Yu, An efficient rhodamine thiospirolactam-based fluorescent probe for detection of Hg^{2+} in aqueous samples, *Analyst*, 2012,**137**, 932.

[S4] N. Wanichacheva, P. Kumsorn, R. Sangsuwan, A. Kamkaew, V. S. Lee, K. Grudpan, A new fluorescent sensor bearing three dansyl fluorophores for highly sensitive and selective detection of mercury(II) ions, *Tetrahedron Lett.*, 2011, **52**, 6133.

[S5] C.-C. Huang, Z. Yang, K.-H. Lee, and H.-T. Chang, Synthesis of highly fluorescent gold nanoparticles for sensing mercury (II), *Angew. Chem. Int. Ed.*, 2007, **46**, 6824

[S6] C. Guo and J. Irudayaraj, Fluorescent Ag clusters via a protein-directed approach as a Hg (II) ion sensor, *Anal. Chem.*, 2011, **83**, 2883

[S7] S. Guha, S. Roy, A. Banerjee, Fluorescent Au@ Ag core–shell nanoparticles with controlled shell thickness and Hg^{II} sensing, *Langmuir*, 2011, **27**, 13198

[S8] Y. Long, D. Jiang, X. Zhu, J. Wang, F. Zhou, Trace Hg^{2+} Analysis via Quenching of the Fluorescence of a CdS-Encapsulated DNA Nanocomposite, *Anal. Chem.*, 2009, **81**, 2652.

[S9] T. Li, Y. Zhou, J. Sun, D. Tang, S. Guo, X. Ding, Electrochemical sensors based on graphene materials, *Microchim. Acta*, 2011, **175**, 113.

[S10] S. Sahu, B. Behera, T. K. Maiti, S. Mohapatra, Simple one-step synthesis of highly luminescent carbon dots from orange juice: application as excellent bio-imaging agents, *Chem. Commun.*, 2012, **48**, 8835.

[S11] X. Jia, J. Li, E. Wang, One-pot green synthesis of optically pH-sensitive carbon dots with upconversion luminescence, *Nanoscale*, 2012, **4**, 5572.

[S12] W. Lu, X. Qin, S. Liu, G. Chang, Y. Zhang, Y. Luo, A. M. Asiri, A. O. Al-Youbi, X. Sun, *Anal. Chem.*, 2012, **84**, 5351.